



Title	Measurement of saturation processes in glutamatergic and GABAergic synapse densities during long-term development of cultured rat cortical networks
Author(s)	Ito, Daisuke; Komatsu, Takumi; Gohara, Kazutoshi
Citation	Brain research, 1534, 22-32 https://doi.org/10.1016/j.brainres.2013.08.004
Issue Date	2013-10-09
Doc URL	http://hdl.handle.net/2115/54524
Type	article (author version)
File Information	HUSCAP_ito_brain res2013.pdf



[Instructions for use](#)

Title:

Measurement of saturation processes in glutamatergic and GABAergic synapse densities during long-term development of cultured rat cortical networks

Authors' names:

Daisuke Ito^{a,b*}, Takumi Komatsu^b, Kazutoshi Gohara^b

Addresses from which the work originated:

^aDivision of Functional Life Science, Faculty of Advanced Life Science, Hokkaido University, North 10, West 8, Kita-ku, Sapporo 060-0810, Japan

^bDivision of Applied Physics, Faculty of Engineering, Hokkaido University, North 13, West 8, Kita-ku, Sapporo 060-8628, Japan

***Corresponding author.**

Present Address: Division of Functional Life Science, Faculty of Advanced Life Science, Hokkaido University, North 10, West 8, Kita-ku, Sapporo 060-0810, Japan; Tel/Fax number: +81-11-706-2985; e-mail; ditoh@mail.sci.hokudai.ac.jp

Abstract

The aim of this study was to clarify the saturation processes of excitatory and inhibitory synapse densities during the long-term development of cultured neuronal networks. For this purpose, we performed a long-term culture of rat cortical cells for 35 days *in vitro* (DIV). During this culture period, we labeled glutamatergic and GABAergic synapses separately using antibodies against vesicular glutamate transporter 1 (VGluT1) and vesicular transporter of γ -aminobutyric acid (VGAT). The densities and distributions of both types of synaptic terminals were measured simultaneously. Observations and subsequent measurements of immunofluorescence demonstrated that the densities of both types of antibody-labeled terminals increased gradually from 7 to 21-28 DIV. The densities did not show a further increase at 35 DIV and tended to become saturated. Triple staining with VGluT1, VGAT, and microtubule-associated protein 2 (MAP2) enabled analysis of the distribution of both types of synapses, and revealed that the densities of the two types of synaptic terminals on somata were not significantly different, but that glutamatergic synapses predominated on the dendrites during long-term culture. However, some neurons did not fall within this distribution, suggesting differences in synapse distribution on target neurons. The electrical activity also showed an initial increase and subsequent saturation of the firing rate and synchronized burst rate during long-term culture, and the number of days of culture to saturation from the initial increase followed the same pattern under this culture condition.

Key words:

Dissociated culture, Immunofluorescence staining, VGluT1, VGAT, multi-electrode arrays.

Abbreviations

CLSM, confocal laser scanning microscopy; DIV, days *in vitro*; DMEM, Dulbecco's modified Eagle's medium; FBS, fetal bovine serum; MAP2, microtubule-associated protein 2; MEA, multi-electrode array; MED, multi-electrode dish; PBS, phosphate-buffered saline; SD, standard deviation; VGAT, vesicular transporter of γ -aminobutyric acid; VGluT1, vesicular glutamate transporter 1.

1. Introduction

Previous studies using animal models and acute slices of brain tissue have revealed many mechanisms associated with nervous system development and functioning (Buzsáki and Draguhn, 2004; Takahashi et al., 2012). *In vitro* culture systems have also contributed to the elucidation of molecular and cellular mechanisms (Fischer et al., 2000; Okabe et al., 2001). The biggest advantage of using a neuronal culture is that it is simpler than analysis using acute slices of tissue (Brewer, 1997; Banker and Goslin, 1998). In addition, cultured neurons enable the long-term and continuous monitoring of the development and maturation of neuronal networks (Lesuisse and Martin, 2002; Opitz et al., 2002). Cultured neuronal systems have therefore been used to investigate synaptic formation in detail (Fletcher et al., 1991; Benson and Cohen, 1996). In addition, by combining the

results of neuronal culture with the recording of electrical activity, the relationships between synapse formation and neuronal activity have been clarified. For example, the measurement of intracellular calcium dynamics has revealed that the frequency of calcium oscillations correlates with the number of synapses in cultured cortical neuronal networks up to 21 days *in vitro* (DIV; Muramoto et al., 1993). Brewer et al. (2009) have also revealed that the network activity recorded using multi-electrode arrays (MEAs) was correlated with synaptophysin-immunopositive density in the development of cultured hippocampal neuronal networks up to 21 DIV (Brewer et al., 2009). However, these previous studies focused mainly on early synaptic formation during early network construction. Network activity is known to show a mature pattern of synchronized bursting after random spontaneous activity in long-term culture (Kamioka et al., 1996; van Pelt et al., 2004; Chiappalone et al., 2006; Wagenaar et al., 2006). During this long-term development, however, how sufficient synaptic connections are established and how the density becomes saturated remain unclear. In addition, excitatory and inhibitory synapses have not been measured directly during this process.

The aim of this study was to assess excitatory and inhibitory synapses separately during the long-term development of cultured neuronal networks. For this purpose, we cultured primary neurons derived from rat cortices for 35 DIV. We constructed a simultaneous measurement system to investigate the densities and distributions of glutamatergic and GABAergic synapses using antibodies against vesicular glutamate transporter 1 (VGluT1) and vesicular transporter of γ -aminobutyric acid (VGAT; Miyazaki et al., 2003; Miura et al., 2006). We show the time-course increases and

saturation for both synaptic densities. In addition, we performed simultaneous staining with VGluT1, VGAT, and microtubule-associated protein 2 (MAP2). Based on the results, we describe the distribution of both synaptic connections on target neurons during long-term culture.

2. Results

2.1. Immunofluorescence staining with MAP2, VGAT, and VGluT1

To observe glutamatergic and GABAergic synapses in cultured neuronal networks both simultaneously and separately, we performed immunofluorescence staining with VGluT1 and VGAT at 3, 7, 14, 21, 28, and 35 DIV. Then, fluorescence observation was performed by confocal laser scanning microscopy (CLSM) to identify the localization of proteins in three dimensions. Figure 1 shows fluorescence micrographs of the cultured cortical cells at 3 DIV. The neuronal neurites began to elongate from the cell somata, and one neurite seemed to become an axon at 3 DIV in DIC micrographs (Fig. 1A, short arrows). MAP2 immunoactivity was not detected at the edge of neurites, but remained in the axon at this time point (Fig. 1B). Some neurons showed VGAT immunoactivity in a region of the soma cytoplasm and one neurite elongated from this soma region (this was considered to be an axon; Fig. 1C-F). At 7 DIV, both VGluT1 and VGAT labeling began to be observed (Fig. 2; a 3D micrograph is shown in Supplemental Movie 1). A series of VGAT-immunopositive punctae was also observed at 7 DIV. At 14 DIV, VGluT1 and VGAT immunoactivities were observed as synaptic bouton-like structures around the MAP2-immunopositive somata and dendrites. At 21 DIV, many VGluT1- and

VGAT-labeled terminals were clearly identified and localized on neurons (the 3D micrograph is shown in Supplemental Movie 2). At 28 and 35 DIV, many more presynaptic terminals (both VGluT1- and VGAT-immunopositive) were labeled on MAP2-positive somata and dendrites (a 3D micrograph for the results at 35 DIV is shown in Supplemental Movie 3). These results indicate that glutamatergic and GABAergic terminals were gradually established and localized on target neurons during the long-term development of cultured neuronal networks.

2.2. Measurement of VGluT1- and VGAT-immunopositive terminals

Using CLSM micrographs, we counted the numbers of VGluT1- and VGAT-immunopositive terminals separately at 7, 14, 21, 28, and 35 DIV. In this experiment, we determined the densities of both types of terminals on somata and dendrites. Figure 3A shows the developmental changes in VGluT1- and VGAT-labeled terminal densities on somata over 35 DIV (the numbers of analyzed neurons at 7, 14, 21, 28, and 35 DIV were 64, 61, 47, 48, and 36, respectively). The density of VGluT1-labeled terminals increased gradually up to 28 DIV (the increases were statistically significant by two-way ANOVA [$F(4, 66) = 85.6, p < 0.005$] and *post hoc* Tukey-Kramer test at 7, 14, and 28 DIV; Table 1). The densities then decreased slightly between 28 and 35 DIV ($p = 0.027$), but did not vary significantly after 35 DIV culture (data not shown). For each value, the data showed large deviations as the network grew. The density of VGAT-labeled terminals on soma did not vary significantly up to 21 DIV ($p = 0.330$ for the comparison between 7 and 14 DIV, and $p = 0.995$ for the comparison between 14 and 21 DIV), but increased

significantly at 28 DIV ($p < 0.005$). The density showed no further increase at 35 DIV ($p = 1$). Significant differences between the densities of VGluT1- and VGAT-labeled terminals were not observed at 7, 14, or 35 DIV, whereas VGluT1 terminals predominated over VGAT terminals at 21 and 28 DIV (two-way ANOVA: $F(1,466) = 24.6$, $p < 0.005$; results of the *post hoc* Tukey-Kramer test are shown in Table 2). These findings indicate that the densities of both glutamatergic and GABAergic terminals on somata became saturated over the first month of development after their initial formation and then increased in density under this culture condition. In addition, the glutamatergic and GABAergic terminals on somata were evenly distributed at 1 month of culture, although the glutamatergic terminals predominated at 21 and 28 DIV.

Figure 3B shows developmental changes in both types of terminals on dendrites ($n = 18$ areas of 6 independent cultures in all DIVs). The density of VGluT1-labeled terminals increased gradually up to 21 DIV (two-way ANOVA: $F(4,170) = 87.27$, $p < 0.005$; *post hoc* Tukey-Kramer test: significant differences were observed in all comparisons; Table 1); however, the densities did not increase at 28 or 35 DIV ($p = 1$ for both). The density of VGAT-labeled terminals increased moderately up to 28 DIV (significant differences were observed except for the comparison of 7 and 14 DIV). VGAT density did not vary significantly at 35 DIV ($p = 0.485$). For each value, both sets of data showed large deviation as the network grew. A comparison of the densities of VGluT1- and VGAT-labeled terminals showed that VGluT1 terminals predominated over VGAT terminals after 14 DIV (two-way ANOVA [$F(1,170) = 79.69$, $p < 0.005$] and *post hoc* Tukey-Kramer test; Table 2). These results indicate that the densities of both types of

terminals on dendrites became saturated over the first month of development after the initial increase in the density of synapses under this culture condition. Moreover, the glutamatergic terminals on dendrites formed more rapidly than the GABAergic terminals, and predominated over the GABAergic terminals over the 1-month culture period.

Cortical neurons did not always show the same distribution of synapses to target cells. Figure 4 demonstrates examples of other cases. For one neuron (white arrow), many VGluT1-labeled and VGAT-labeled terminals were distributed on both soma and dendrites. Another neuron (yellow arrow) had few VGluT1-labeled terminals on the somata and many VGAT-labeled terminals on both somata and dendrites (the 3D distribution is shown in Supplemental Movie 4). These results suggest that the distributions of glutamatergic and GABAergic synapses on target neurons were not homogeneous, but rather that differences in synaptic distribution existed among the individual neurons under this culture condition. The large deviations in terminal densities observed in Fig. 3 are attributed to these heterogeneous distributions.

2.3. Electrical activity recordings

Cortical cells were cultured on MEAs, and spontaneous electrical activity was recorded at 7, 10, 14, 17, 21, 28, 31, and 35 DIV (n = 6 cultures; Fig. 5AB). In agreement with previous studies (Kamioka et al., 1996; van Pelt et al., 2004), we observed that the spontaneous spikes became synchronized bursts during the development of neuronal networks (Fig. 5B). Figure 5C shows developmental changes in the array-wide firing rate (number of spikes per second summed over all electrodes) and synchronized burst rate.

The first measurement of spikes was made at 7 DIV. The mean firing rate increased at each time point up to and including 31 DIV, but significant differences in the mean firing rate were not observed until 28 DIV (Tukey-Kramer test followed by one-way ANOVA [$F(7) = 17.5$, $p < 0.005$]; Table 3). Although no statistically significant difference was observed between 21 and 28 DIV ($p = 0.130$), the firing rate at 28 DIV was different from the rate at each of the time points before 17 DIV ($p < 0.005$). The firing rate did not increase significantly at 31 and 35 DIV. Synchronized bursts were observed at 14 DIV and the subsequent time points. The synchronized burst rate increased up to 31 DIV, but significant differences were not observed until 28 DIV, just as for the firing rate (Tukey-Kramer test followed by one-way ANOVA [$F(7) = 23.9$, $p < 0.005$]; Table 3). Although the burst rate was not significantly different between 21 and 28 DIV ($p = 0.057$), the burst rate at 28 DIV was different from the rate at each of the time points before 17 DIV ($p < 0.005$), just as for the firing rate. The burst rate also did not increase significantly at 31 and 35 DIV. The trend was similar to that for the change in the firing rate. These results indicate that network activity (firing rate and synchronized burst rate) became saturated at 28 DIV after the initial increase and remained saturated thereafter under this culture condition.

3. Discussion

3.1. Saturation of VGluT1- and VGAT-immunopositive synaptic densities during long-term culture

In the present study, we cultured cortical neurons for 35 DIV. We then performed

immunofluorescence staining to label the glutamatergic and GABAergic synapses simultaneously using antibodies against VGluT1 and VGAT. Previous studies have focused mainly on the early development of neuronal networks, particularly on early synaptic formation up to 18-21 DIV (Muramoto et al., 1993; Benson et al., 1996; Brewer et al., 2009). Therefore, we assessed the long-term synaptic changes. The densities of glutamatergic and GABAergic terminals became saturated at 28-35 DIV after initially increasing between 7 and 28 DIV (glutamatergic synapses on dendrites became saturated earlier, at 21 DIV). These results demonstrated not only development but also maturation of neuronal networks during long-term culture under this culture condition. Brewer et al. (2009) revealed that NbActiv4 medium, an improved version of Neurobasal/B27 medium, increased the synapse density. Therefore, it is considered that the cellular or synaptic requirements change as the DIV increases. Since the culture medium might be one of limiting factors on synapse saturation, it will be necessary to confirm the saturation process using other culture conditions.

Previous molecular biological studies have identified three subtypes of VGluT: VGluT1, VGluT2, and VGluT3 (Ni et al., 1994; Aihara et al., 2000; Gras et al., 2002). Glutamatergic neurons express at least one of these three VGluTs. In the adult brain, VGluT1 predominates in the cerebral cortices and hippocampus, whereas VGluT2 expression is predominant in the diencephalon, brainstem, and spinal cord (Fremeau et al., 2001; Herzog et al., 2001; Wojcik et al., 2004). However, none of these brain regions exclusively expresses one isoform. VGluT3 is less widely expressed than the other two (Grass et al., 2002). In mammalian development, VGluT1 expression increases gradually

after birth and predominates over the other isoforms in telencephalic regions. In contrast, VGluT2 is expressed at high levels shortly after birth and declines with age (Boulland et al., 2004; Nakamura et al., 2005). In the present study, we only investigated the changes in VGluT1-immunopositive synapse densities. Our results (the VGluT1-positive puncta became saturated after a gradual increase) resemble those for mammalian development. However, VGluT2 and VGluT3 immunoactivity should be investigated to clarify the saturation process of glutamatergic synapses, although VGluT1 synapses were considered to be predominant over VGluT2 synapses in the cerebral cortex samples we used.

At the early stages, VGAT immunolabeling was detected in the cytoplasm region adjacent to the nucleus and in specific neurites in some neurons (Fig. 1). The localization of presynaptic proteins in the soma and neurites was also previously demonstrated for synapsin 1 and synaptophysin (Fletcher et al., 1991; Benson and Cohen, 1996). In the present study, the VGAT positivity was considered to reflect axonal transport of the VGAT protein from the Golgi apparatus (see Fig. 1). At 7 DIV, both VGluT1- and VGAT-labeled punctae began to be observed around the MAP2-immunopositive neurons, and both types of terminals were clearly identified from 14 to 35 DIV using these antibodies (Fig. 2). Such simultaneous staining with VGluT1 and VGAT allowed separate analysis of the densities of glutamatergic and GABAergic synaptic terminals in cultured neuronal networks during long-term development.

3.2. Distribution of glutamatergic and GABAergic synapses during long-term culture

The triple-staining, CLSM observation and quantitative analysis methods used in

this study also enabled analysis of the distributions of glutamatergic and GABAergic synaptic terminals on target neurons. The results showed that glutamatergic and GABAergic terminals were distributed equally on the somata, whereas glutamatergic terminals predominated on dendrites (Fig. 3), although some neurons did not show this pattern (Fig. 4). Excitatory and inhibitory synapses are differentially distributed on target neurons in the hippocampus and neocortex (Gray, 1959; Blackstad and Flood, 1963; Andersen et al., 1966). These different distributions of excitatory and inhibitory synapses have also been demonstrated in hippocampal cultures using antibodies against synaptophysin and GAD65 (Benson and Cohen, 1996; Benson and Tanaka, 1998). Some neurons received the GABAergic inputs mostly on somata (Fig. 5), and this distribution is consistent with *in vivo* data and previous work using hippocampal neurons. These data suggest that the distributions of glutamatergic and GABAergic terminals differ from cell to cell during long-term culture. Previous studies using dissociated cultures and MEAs revealed that cultured neuronal networks retain a self-organized topology (Eytan and Marom, 2006; Paquale et al., 2008), which implies heterogeneous distributions in excitatory and inhibitory synapses. Therefore, it is necessary to investigate the distributions of glutamatergic and GABAergic synapses in the region of target cells and individual neurons experimentally based on electrical activity to clarify these heterogeneous distributions in detail.

3.3. Relationship between synaptic densities and network electrical activity in long-term culture

Taking advantage of MEA-based recording for neuronal network activity, we also measured the electrical activity of cultured cortical networks (Thomas et al., 1972; Gross et al., 1977; Pine, 1980). The networks showed synchronized bursts, and the network activity (firing rate and synchronized burst rate) became saturated, with large deviations, after initially increasing during the 1-month culture period under this culture condition (Fig. 5BC). This indicates that we successfully observed the process of network maturation via early development. Previously, we reported that the densities of surviving neurons at 35 DIV decreased dramatically to approximately 150 neurons/mm² (initially plated at 2500 cells/mm²) under these culture conditions (Ito et al., 2010). The rate of surviving neurons might also contribute to increases and eventual saturation of the firing rate and burst rate. The counting of surviving neurons at each culture DIV will also be required to determine the saturation of network activity.

The tendencies of the changes in firing rate and synchronized burst rate were similar to the changes in both types of synaptic densities under this culture condition. Brewer et al. (2009) revealed that network activity correlates with synaptophysin-immunopositive density during early development (up to 21 DIV; Brewer et al., 2009). Therefore, these results also imply that the relationship between synaptic densities and network electrical activity occurs even in mature processes. However, the culture conditions differed between measurements for both types of synapses and measurements for electrical activity in this study. As described above, the culture medium used in this experiment might have been one of limiting factors on the saturation. The number of surviving neurons might also have contributed to the measured network

activity. Therefore, in examining the relation between synapse saturation and network activity, many factors should be taken into consideration, such as the firing properties of each neuron, the neuron morphology, the numbers of neurite branches and astrocytes, the condition of the spine, the synaptic plasticity, and the gene/protein expression levels. Appropriately designed experiments will thus be needed to identify each of the limiting factors. For example, direct immunofluorescence staining on MEAs allows analysis of the spatial factors that affect electrical activity (Ito et al., 2010; Maccilone et al., 2010), and could be of use in this context. However, observing small objects, such as synaptic proteins, directly on MEAs is difficult because of the thickness of the MEA substrate. When this problem is overcome, the triple staining and analysis of 3D reconstructed images used in this study will contribute to our understanding of the neuronal network dynamics.

After the initial development in the mammalian brain, synapse elimination and refinement occur through interaction with the environment via sensory inputs (Huttenlocher et al., 1982; Elston et al., 2009). However, the detailed mechanisms of this elimination and refinement remain unclear. Cultured neuronal networks, which were used in this study, do not receive external inputs, and it is not difficult to stimulate cultured neuronal networks at any site through MEAs (Jimbo et al., 1999; Wagenaar et al., 2005; Chiappalone et al., 2008). Therefore, it is important to determine whether synaptic elimination and refinement will occur in cultured neuronal networks receiving mimic sensory inputs via MEAs based on the present results. Further studies will be needed to clarify the mechanisms underlying synaptic elimination and refinement.

4. Experimental procedures

4.1. Cell culture

We cultured cortical cells derived from Wistar rats at embryonic day 17 using a Nerve-Cell Culture System (Sumitomo Bakelite Co., Tokyo, Japan) as described previously (Ito et al., 2010; Yamaguchi et al., 2011; Uchida et al., 2012; Suzuki et al., 2013). Cortices of 2 rats were dissociated into single cells using dissociation solution (Sumitomo Bakelite Co.), then resuspended in Neuron Culture Medium (serum-free conditioned medium from 48-h rat astrocyte confluent cultures based on Dulbecco's modified Eagle's medium [DMEM]/F-12 with N2 supplement; Sumitomo Bakelite; Takeuchi et al., 2005). The cell suspension was plated onto poly(ethyleneimine)-coated 13 ϕ coverslips, which were inserted into 24-well cell culture plates at a density of 250 cells/mm² for immunofluorescence staining. We also plated the cell suspension onto a poly(ethyleneimine)-coated multi-electrode dish (MED) probe (Alpha MED Scientific, Osaka, Japan), which consisted of 64 planar microelectrodes (MED-p515A) at a density of 2500 cells/mm² for electrical activity recordings. The total cell numbers were the same on the coverslips and the MED probe. The cultures were incubated with the above-described Neuron Culture Medium in a humidified atmosphere containing 5% CO₂ and 95% air at 37 \square . After 3 days of culture, half of the culture medium was replaced with fresh medium consisting of DMEM (Life Technologies-Gibco, Carlsbad, CA) supplemented with 5% fetal bovine serum (FBS; Life Technologies-Gibco), 5% horse

serum (Sigma-Aldrich, St. Louis, MO), 25 $\mu\text{g}/\text{mL}$ insulin (Life Technologies-Gibco), 100 U/mL penicillin, and 100 $\mu\text{g}/\text{mL}$ streptomycin (Life Technologies-Gibco). Then, half of the culture medium was replaced at 7, 10, 14, 17, 21, 24, 28, and 31 DIV. Immunofluorescence staining was performed at 3, 7, 14, 21, 28, and 35 DIV. Electrical activity recordings were performed at 7, 10, 14, 17, 21, 28, 31, and 35 DIV before the culture medium was replaced. For immunofluorescence staining, three independent cultures were prepared for each time point. To measure the synapse densities at six different time points, we prepared 18 independent cultures initially. For electrical activity recordings, three MED probes were used. These overall cultures for 35 DIV were repeated twice. Thus, 6 independent cultures on coverslips for one time point and 6 independent cultures on MED probes from 4 rats were performed.

4.2. Immunofluorescence staining and confocal laser scanning microscopy (CLSM)

The primary antibodies were anti-MAP2 mouse IgG (1:500; Sigma-Aldrich), anti-VGluT1 rabbit IgG (1:1000; Frontier Institute Co., Hokkaido, Japan), and anti-VGAT guinea pig IgG (1:1000; Frontier Institute Co.). The secondary antibodies were Alexa Fluor 405-labeled anti-mouse IgG (Life Technologies-Molecular Probes), Alexa Fluor 488-labeled anti-guinea pig IgG, and Alexa Fluor 546-labeled anti-rabbit IgG.

The cultures on coverslips were fixed with 4% formaldehyde in phosphate-buffered saline (PBS; Life Technologies-Gibco) for 10 min at 3, 7, 14, 21, 28, and 35 DIV. After permeabilization with 0.5% Triton X-100 in PBS for 10 min, the

cultures were incubated with PBS containing 10% goat serum and 0.01% Triton X-100 for 30 min. The permeabilized cultures were incubated with primary antibodies in PBS containing 10% goat serum overnight at 4°C and were rinsed with PBS for 10 min three times. The cultures were then incubated with secondary antibodies (0.4% in PBS containing 10% goat serum) for 1 h at room temperature and rinsed three additional times. The coverslips were removed from the 24-well plate and mounted. Fluorescence images were acquired using a confocal laser-scanning unit (FV1000-D; Olympus, Tokyo, Japan) coupled to an IX-81 microscope (Olympus) from 35-45 serial images (thickness, 0.43 µm). Together, they covered a distance of approximately 15-20 µm on the z-axis (according to cell size). Each optical section was obtained at a spatial sampling of 248 nm/pixel (512×512 pixels) through an Olympus UPLAPO 100×/1.35 oil immersion objective. Images projected onto one plane are shown in this paper. Differential interference contrast (DIC) images were also captured.

4.3. Quantitative image analysis

Velocity 5.5.1 visualization and quantification software (PerkinElmer, Waltham, MA) was used to reconstruct three-dimensional (3D) images and for quantitative analysis. After reconstruction, background noise was removed using a median filter. Each VGluT1- and VGAT-immunopositive puncta was detected as a spherical object by setting a brightness intensity threshold. After automatically separating objects that were touching, oversized and small objects were excluded. Object area limits were set at 0.05-10 µm³. Next, the number of objects was counted. The MAP2-immunoactive area was also

quantified. Detection of the MAP2-immunopositive area was conducted by setting a brightness intensity threshold, and the volume of this area was calculated. The densities of the VGluT1- and VGAT-labeled terminals were defined as the number of VGluT1- and VGAT-immunopositive punctae per MAP2-immunopositive area. The excitatory and inhibitory synaptic terminals were differentially distributed on their postsynaptic target cells in the hippocampus and neocortex (Gray, 1959; Blackstad and Flood, 1963; Andersen et al., 1966). We therefore determined the densities of both types of terminals on somata and dendrites separately. The cell somata in each immunofluorescence micrograph were selected manually and clipped out. The clipped area included both the VGluT1- and VGAT-immunopositive punctae. The densities of both types of terminals on somata were defined as their densities in this clipped area, while the densities of these terminals on dendrites were defined as their densities outside of the clipped area.

4.4. Electrophysiology

Spontaneous electrical activity recordings were performed using a MED64 extracellular recording system (Alpha MED Scientific) at a sampling rate of 20 kHz with a software filter (MED Mobius; Alpha MED Scientific) set to 100-5000 Hz for 300 s. All recordings were conducted in an incubator at 37°C. After recording, the cultures were returned to the CO₂ incubator. Activity was recorded approximately twice per week for 35 DIV.

The amplitudes of what we considered to be spikes had to exceed a noise-based threshold within a window of 1 ms. Threshold determination was performed as described

previously (Ito et al., 2010; Uchida et al., 2012). Synchronized bursts were defined as described below (Ito et al., 2010). The time window was set to 100 ms and then the spikes (total for all electrodes) in the window were counted. By shifting the window, a histogram of the change in firing rate across the threshold was obtained for each culture. Anything above the threshold was defined as a synchronized burst. The threshold was set to 100 spikes per window.

4.5. Statistical analysis

Data are shown as the mean \pm SD. Statistically significant differences for synapse densities were evaluated by two-way ANOVA with *post hoc* Tukey-Kramer to test for the effect of time and whether the two types of synapse densities were different from each other; and those for electrophysiological data were evaluated by one-way ANOVA with *post hoc* Tukey-Kramer. Probability values less than 0.05 were considered to indicate statistical significance.

Acknowledgements

This work was supported in part by Grants-in-Aid for Scientific Research from the Japan Society for the Promotion of Science awarded to K. Gohara (Nos. 20240023 and 21650049) and to D. Ito (Nos. 23700523 and 24 • 3395). We are grateful to Prof. M. Watanabe (Hokkaido University School of Medicine, Sapporo, Japan) for kindly providing us with the antibodies against VGluT1 and VGAT.

References

- Aihara, Y., Mashima, H., Onda, H., Hisano, S., Kasuya, H., Hori, T., Yamada, S., Tomura, H., Yamada, Y., Inoue, I., Kojima, I., Takeda, J., 2000. Molecular cloning of a novel brain-type Na(+)-dependent inorganic phosphate cotransporter. *J. Neurochem.* 74, 2622-2625.
- Andersen, P., Blackstad, T.W., Lömo, T., 1966. Location and identification of excitatory synapses on hippocampal pyramidal cells. *Exp. Brain Res.* 1, 236-248.
- Banker, G., Goslin, K., 1998. Types of nerve cell cultures, their advantages and limitations. In Banker, G. & Goslin, K. (eds), *Culturing Nerve Cells*, 2nd edition. MIT Press, Cambridge, MA, 11-36.
- Benson, D.L., Cohen, P.A., 1996. Activity-independent segregation of excitatory and inhibitory synaptic terminals in cultured hippocampal neurons. *J. Neurosci.* 16, 6424-6432.
- Benson, D.L., Tanaka, H., 1998. N-Cadherin redistribution during synaptogenesis in hippocampal neurons. *J. Neurosci.* 18, 6892-6904.
- Blackstad, T.W., Flood, P.R., 1963. Ultrastructure of hippocampal axosomatic synapses. *Nature* 198, 542-543.
- Boulland, J.L., Qureshi, T., Seal, R.P., Rafiki, A., Gundersen, V., Bergersen, L.H., Fremeau JR., R.T., Edwards, R.H., Storm-Mathisen, J., Chaudhry, F.A., 2004. Expression of the vesicular glutamate transporters during development indicates the widespread corelease of multiple neurotransmitters. *J. Comp. Neurol.* 480, 264-280.

- Brewer, G.J., 1997. Isolation and culture of adult rat hippocampal neurons. *J. Neurosci. Meth.* 71, 143-155.
- Brewer, G.J., Boehler, M.D., Pearson, R.A., DeMaris, A.A., Ide, A.N., Wheeler, B.C., 2009. Neuron network activity scales exponentially with synapse density. *J. Neural Eng.* 6, 014001.
- Buzsáki, G., Draguhn, A., 2004. Neuronal oscillations in cortical networks. *Science* 304, 1926-1929.
- Chiappalone, M., Bove, M., Vato, A., Tedesco, M., Martinoia, S., 2006. Dissociated cortical networks show spontaneously correlated activity patterns during *in vitro* development. *Brain Res.* 1093, 41-53.
- Chiappalone, M., Massobrio, P., Martinoia, S., 2008. Network plasticity in cortical assemblies. *Eur. J. Neurosci.* 28, 221-237.
- Elston, G.N., Oga, T., Fujita, I., 2009. Spinogenesis and pruning scales across functional hierarchies. *J. Neurosci.* 29, 3271-3275.
- Eytan, D., Marom, S., 2006. Dynamics and effective topology underlying synchronization in networks of cortical neurons. *J. Neurosci.* 26, 8465-8476.
- Fischer, M., Kaech, S., Wagner, U., Brinkhaus, H., Matus, A., 2000. Glutamate receptors regulate actin-based plasticity in dendritic spines. *Nat. Neurosci.* 3, 887-894.
- Fletcher, T.L., Cameron, P., De Camilli, P., Banker, G., 1991. The distribution of synapsin I and synaptophysin in hippocampal neurons developing in culture. *J. Neurosci.* 11, 1617-1628.
- Freneau, R.T., Troyer, M.D., Pahner, I., Nygaard, G.O., Tran, C.T., Reimer, R.J.,

- Bellocchio, E.E., Fortin, D., Storm-Mathisen, J., Edwards, R.H., 2001. The expression of vesicular glutamate transporters defines two classes of excitatory synapse. *Neuron* 31, 247-260.
- Gras, C., Herzog, E., Bellenchi, G.C., Bernard, V., Ravassard, P., Pohl, M., Gasnier, B., Giros, B., El Mestikawy, S., 2002. A third vesicular glutamate transporter expressed by cholinergic and serotonergic neurons. *J. Neurosci.* 22, 247-260.
- Gray, E.G., 1959. Axo-somatic and axo-dendritic synapses of the cerebral cortex: and electron microscope study. *J. Anat.* 93, 420-433.
- Gross, G.W., Rieske, E., Kreutzberg, G.W., Meyer, A.A., 1977. New fixed-array multi-microelectrode system designed for long-term monitoring of extracellular single unit neuronal activity *in vitro*. *Neurosci. Lett.* 6, 101-105.
- Herzog, E., Bellenchi, G.C., Gras, C., Bernard, V., Ravassard, P., Bedet, C., Gasnier, B., Giros, B., Mestikawy, S.E.I., 2001. The existence of a second vesicular glutamate transporter specifies subpopulations of glutamatergic neurons. *J. Neurosci.* 21, RC181, 1-6.
- Huttenlocher, P.R., de Courten, C., Garey, L.J., Van der Loos, H., 1982. Synaptogenesis in human visual cortex-evidence for synapse elimination during normal development. *Neurosci. Lett.* 33, 247-252.
- Ito, D., Tamate, H., Nagayama, M., Uchida, T., Kudoh, S.N., Gohara, K., 2010. Minimum neuron density for synchronized bursts in a rat cortical culture on multi-electrode arrays. *Neuroscience* 171, 50-61.
- Jimbo, Y., Tatemo, T., Robinson, H.P.C., 1999. Simultaneous induction of

- pathway-specific potentiation and depression in networks of cortical neurons. *Biophys. J.* 76, 670-678.
- Kamioka, H., Maeda, E., Jimbo, Y., Robinson, H.P.C., Kawana, A., 1996. Spontaneous periodic synchronized bursting during formation of mature patterns of connections in cortical cultures. *Neurosci. Lett.* 206, 109-112.
- Lesuisse, C., Martin, L.J., 2002. Long-term culture of mouse cortical neurons as a model for neuronal development, aging, and death. *J. Neurobiol.* 51, 9-23.
- Maccione, A., Gandolfo, M., Tedesco, M., Nieuw, T., Imfeld, K., Martinoia, S., Berdonidini, L., 2010. Experimental investigation on spontaneously active hippocampal cultures recorded by means of high-density MEAs: analysis of the spatial resolution effects. *Front. Neuroeng.* 3, 4.
- Miura, E., Fukaya, M., Sato, M., Sugihara, T., Asano, M., Yoshioka, K., Watanabe, M., 2006. Expression and distribution of JNK/SAPK-associated scaffold protein JSAP1 in developing and adult mouse brain. *J. Neurochem.* 97, 1431-1446.
- Miyazaki, T., Fukaya, M., Shimizu, H., Masahiko, W., 2003. Subtype switching of vesicular glutamate transporters at parallel fibre-Purkinje cell synapses in developing mouse cerebellum. *Eur. J. Neurosci.* 17, 2563-2572.
- Mukai, Y., Shiina, T., Jimbo, Y., 2003. Continuous monitoring of developmental activity changes in cultured cortical networks. *Electr. Eng. Jpn.* 145, 28-37.
- Muramoto, K., Ichikawa, M., Kawahara, M., Kobayashi, K., Kuroda, Y., 1993. Frequency of synchronous oscillations of neuronal activity increases during development and is correlated to the number of synapses in cultured cortical neuron networks. *Neurosci.*

Lett. 163, 163-165.

Nakamura, K., Hioki, H., Fujiyama, F., Kaneko, T., 2005. Postnatal changes of vesicular glutamate transporter (VGluT)1 and VGluT2 immunoreactivities and their colocalization in the mouse forebrain. *J. Comp. Neurol.* 492, 263-288.

Ni, B., Rosteck, P.R. Jr, Nadi, N.S., Paul, S.M., 1994. Cloning and expression of a cDNA encoding a brain-specific Na(+)-dependent inorganic phosphate cotransporter. *Proc. Natl. Acad. Sci. USA.* 91, 5607-5611.

Okabe, S., Miwa, A., Okado, H., 2001. Spine formation and correlated assembly of presynaptic and postsynaptic molecules. *J. Neurosci.* 21, 6105-6114.

Opitz, T., de Lima, A.D., Voigt, T., 2002. Spontaneous development of synchronous oscillatory activity during maturation of cortical networks *in vitro*. *J. Neurophysiol.* 88, 2196-2206.

Pasquale, V., Massobrio, P., Bologna, L.L., Chiappalone, M., Martinoia, S., 2008. Self-organization and neuronal avalanches in networks of dissociated cortical neurons. *Neuroscience* 152, 1354-1369.

Pine, J., 1980. Recording action potentials from cultured neurons with extracellular microcircuit electrodes. *J. Neurosci. Methods* 2, 19-31.

Suzuki, M., Ikeda, K., Yamaguchi, M., Kudoh, S.N., Yokoyama, K., Satoh, R., Ito, D., Nagayama, M., Uchida, T., Gohara, K., 2013. Neuronal cell patterning on a multi-electrode array for a network analysis platform. *Biomaterials* in press.

Takahashi, N., Kitamura, K., Matsuo, N., Mayford, M., Kano, M., Matsuki, N., Ikegaya, Y., 2012. Locally synchronized synaptic inputs. *Science* 335, 353-356.

- Takeuchi, H., Mizuno, T., Zhang, G., Wang, J., Kawanouchi, J., Kuno, R., Suzumura, A., 2005. Neuritic beading induced by activated microglia is an early feature of neuronal dysfunction toward neuronal death by inhibition of mitochondrial respiration and axonal transport. *J. Biol. Chem.* 280, 10444-10454.
- Thomas, C.A., Springer, P.A., Okun, L.M., Berwaldn, Y., Loeb, G.E., 1972. Miniature microelectrode array to monitor bioelectric activity of cultured cells. *Exp. Cell Res.* 74, 61-66.
- Uchida, T., Suzuki, S., Hirano, Y., Ito, D., Nagayama, M., Gohara, K., 2012. Xenon-induced inhibition of synchronized bursts in a rat cortical neuronal network. *Neuroscience* 214, 149-158.
- van Pelt, J., Wolters, P.S., Corner, M.A., Rutten, W.L.C., Ramackers, G.J.A., 2004. Long-term characterization of firing dynamics of spontaneous bursts in cultured neural networks. *IEEE Trans. Biomed. Eng.* 5, 2051-2062.
- Wagenaar, D.A., Madhavan, R., Pine, J., Potter, S.M., 2005. Controlling bursting in cortical cultures with closed-loop multi-electrode stimulation. *J. Neurosci.* 25, 680-688.
- Wagenaar, D.A., Pine, J., Potter, S.M., 2006. An extremely rich repertoire of bursting patterns during the development of cortical cultures. *BMC Neurosci.* 7, 11.
- Wojcik, S.M., Rhee, J.S., Herzog, E., Sigler, A., Jan, R., Takamori, S., Brose, N., Rosenmund, C., 2004. An essential role for vesicular glutamate transporter 1 (VGLUT1) in postnatal development and control of quantal size. *Proc. Nat. Acad. Sci. USA.*, 101, 7158-7163.

Yamaguchi, M., Ikeda, K., Suzuki, M., Kiyohara, A., Kudoh, S.N., Shimizu, K., Taira, T., Ito, D., Uchida, T., Gohara, K., 2012. Cell patterning using a template of microstructured organosilane layer fabricated by vacuum ultraviolet light lithography. *Langmuir* 27, 12521-12532.

Figure Legends

Figure 1

Immunofluorescence micrographs of cortical cultures at 3 DIV. All images were obtained by CLSM. Fluorescence micrographs show projection of the serial images on the *z*-axis. (A) DIC micrograph of a cortical culture. The axon (short arrows) was elongated from the soma (long arrow). Scale bar = 30 μm . (B) Neurons expressing MAP2 (blue). (C) VGAT protein was identified using an antibody against VGAT (green). The dotted circle indicates the localization of VGAT in the cytoplasm. VGAT was also identified in a single neurite (short arrow). (D) Micrograph showing the merging of the three fluorescence images of MAP2 (blue), VGAT (green), and VGluT1 (red). (E) Merged fluorescence images and DIC images. (F) The upper panel shows an *x-z* image of the horizontal line, and the left panel shows a *y-z* image of the vertical line.

Figure 2

Immunofluorescence micrographs of MAP2, VGAT, and VGluT1 in 7, 14, 21, 28, and 35 DIV cultures. The left-hand panels present MAP2 images (blue). The middle panels show

VGAT (green) and VGluT1 (red) images. The right-hand panels display images created by merging the images of MAP2, VGAT, and VGluT1. Scale bar = 30 μ m.

Figure 3

Developmental changes in the densities of VGluT1-labeled terminals and VGAT-labeled terminals during culture for 35 DIV. (A) The densities of VGluT1- and VGAT-labeled terminals on somata. The numbers of analyzed neurons at 7, 14, 21, 28, and 35 DIV were 64, 61, 47, 48, and 36, respectively. (B) The densities of both types of terminals on dendrites. Open red circles represent the density of VGluT1-labeled terminals and filled red circles show the mean density of VGluT1-labeled terminals. $n = 18$ areas of 6 independent cultures in all DIVs. Open triangles indicate the density of VGAT-labeled terminals and filled green triangles denote the mean density of VGAT-labeled terminals. Horizontal jittering was performed for visual clarity. Data are presented as the mean \pm SD.

Figure 4

Examples of heterogeneous distributions of VGluT1- and VGAT-labeled terminals on target neurons. Fluorescence micrographs of cultured cortical cells at 35 DIV. The images are projections of serial images on the z -axis captured by CLSM. (A) Neurons were identified using an anti-MAP2 antibody. (B) GABAergic terminals were identified using an anti-VGAT antibody. (C) Glutamatergic terminals were identified using an anti-VGluT1 antibody. (D) Merging of MAP2, VGAT, and VGluT1. For one neuron (white arrow), many VGluT1-labeled terminals were distributed on both somata and

dendrites (especially on dendrites), and many VGAT-labeled terminals were also distributed on both somata and dendrites. Another neuron (yellow arrowhead) had few VGluT1-labeled terminals on somata and many VGAT-labeled terminals on both somata and dendrites. Scale bar = 30 μm .

Figure 5

Measurement of spontaneous electrical activity in cultured cortical networks for 35 DIV using MEAs. (A) Representative phase-contrast micrograph of cultured cortical cells on MEAs. Each electrode has a size of 50 \times 50 μm . Scale bar = 150 μm . (B) Examples of extracellular potential traces of cultured neuronal networks on MEAs at 7 and 35 DIV. (C) Developmental changes in the array-wide firing rate and synchronized burst rate of cultured cortical networks. Filled circles represent the array-wide firing rate and open triangles indicate the synchronized burst rate ($n = 6$ cultures). Data are presented as the mean+SD (firing rate) and mean-SD (synchronized burst rate).

Table Legends

Table 1

Statistical analysis of VGluT1- and VGAT-immunopositive puncta densities at different time points between 7 and 35 DIV. * $p < 0.05$; ** $p < 0.005$.

Table 2

Statistical analysis of VGluT1- and VGAT-immunopositive puncta densities. * $p < 0.05$;

**** $p < 0.005$.**

Table 3

Statistical analysis of the firing rate and synchronized burst rate at different time points between 7 and 35 DIV. * $p < 0.05$; ** $p < 0.005$.

Supplemental information

Supplemental Movie 1

This movie presents the reconstructed 3D micrograph of cultured cortical neurons at 7 DIV shown in the merged panel of Fig. 3 in all directions.

Supplemental Movie 2

This movie presents the reconstructed 3D micrograph of cultured cortical neurons at 21 DIV shown in the merged panel of Fig. 3 in all directions.

Supplemental Movie 3

This movie presents the reconstructed 3D micrograph of cultured cortical neurons at 35 DIV shown in the merged panel of Fig. 3 in all directions.

Supplemental Movie 4

This movie presents the reconstructed 3D micrograph of cultured cortical neurons at 35 DIV shown in the merged panel of Fig. 4 in all directions.

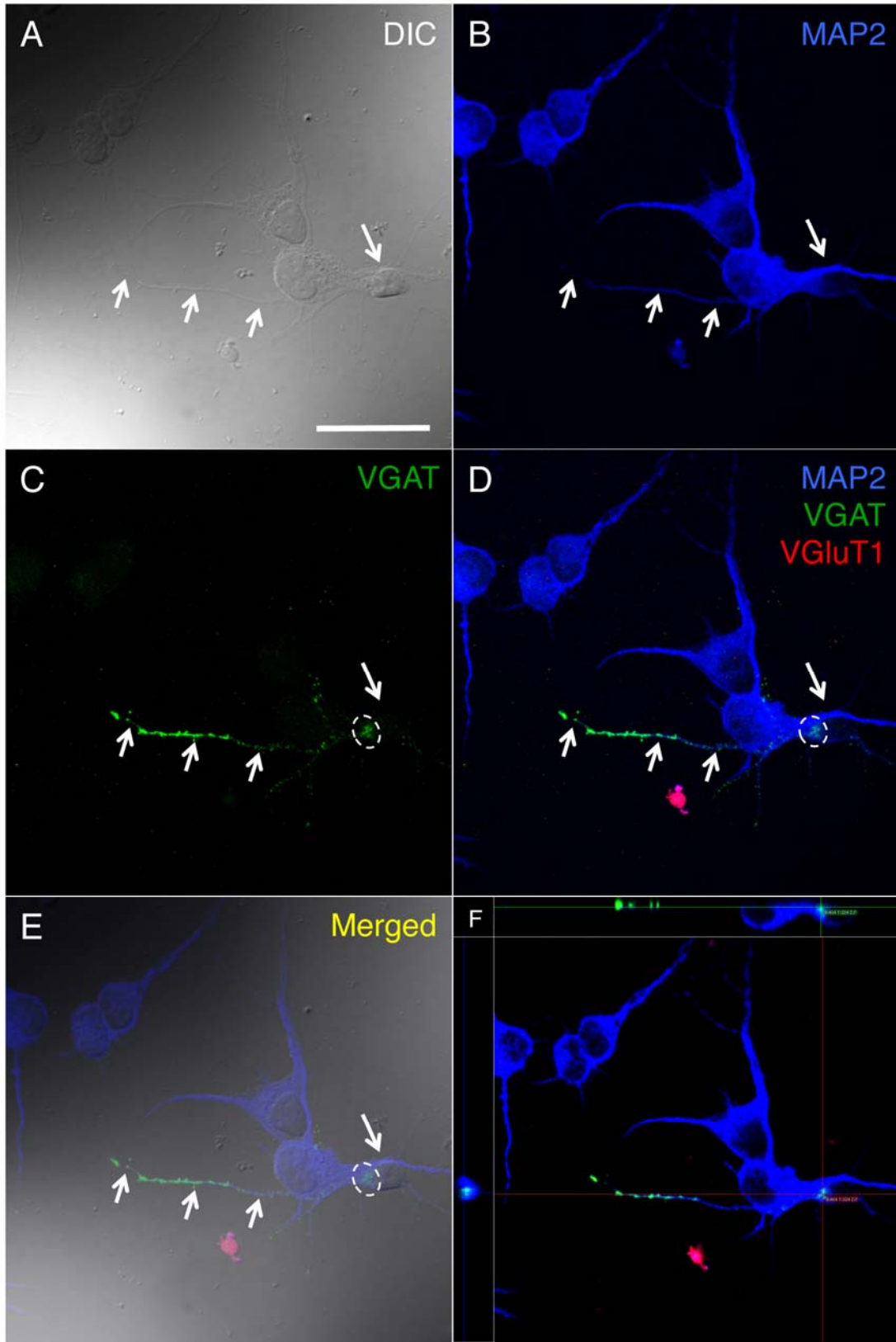


Fig. 1

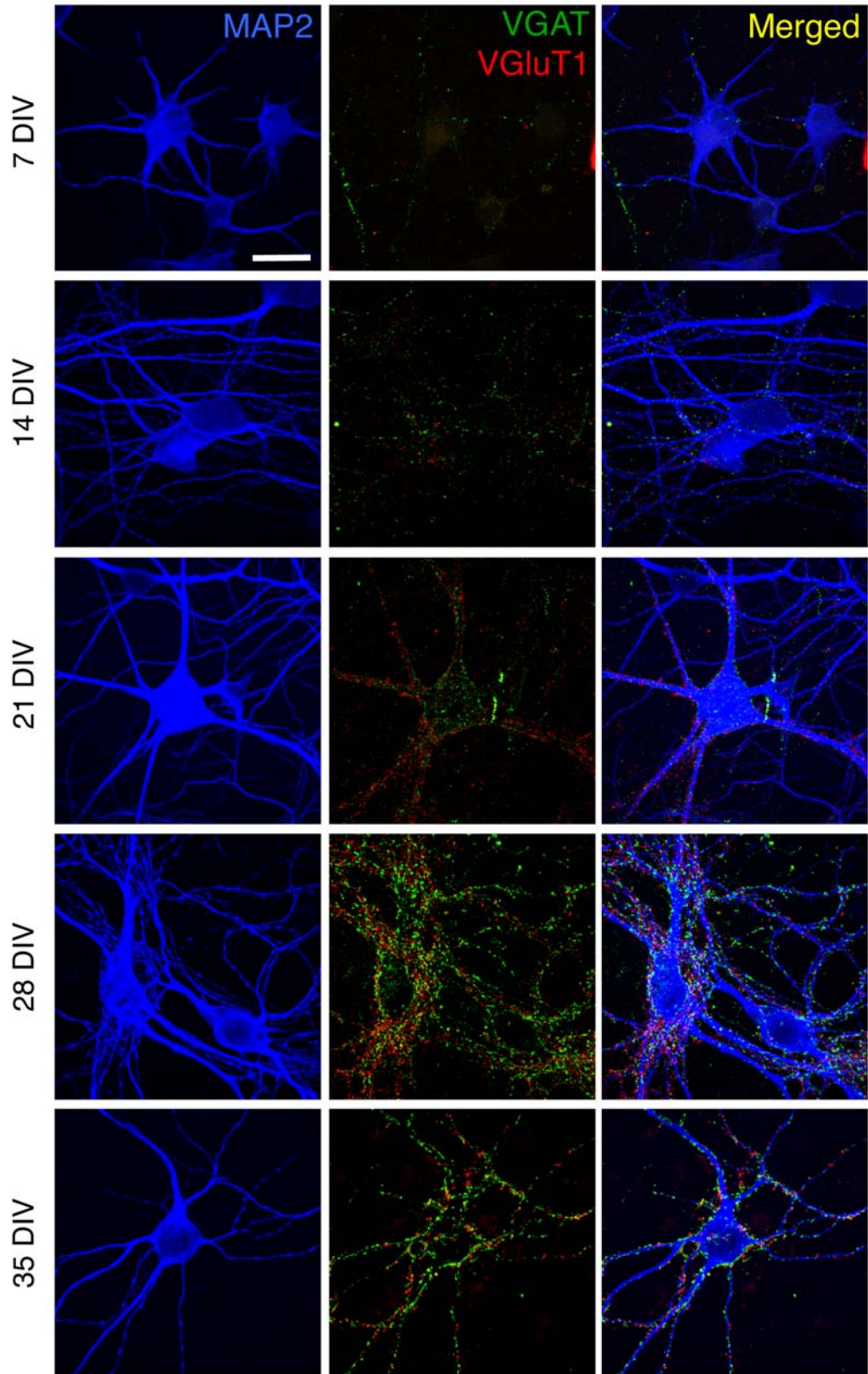


Fig. 2

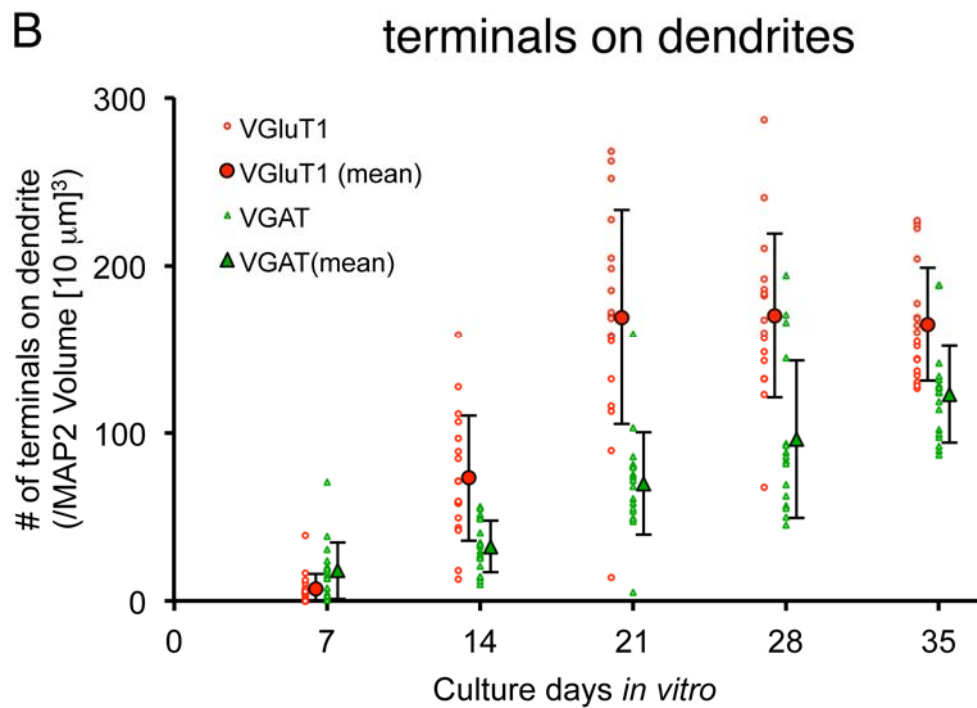
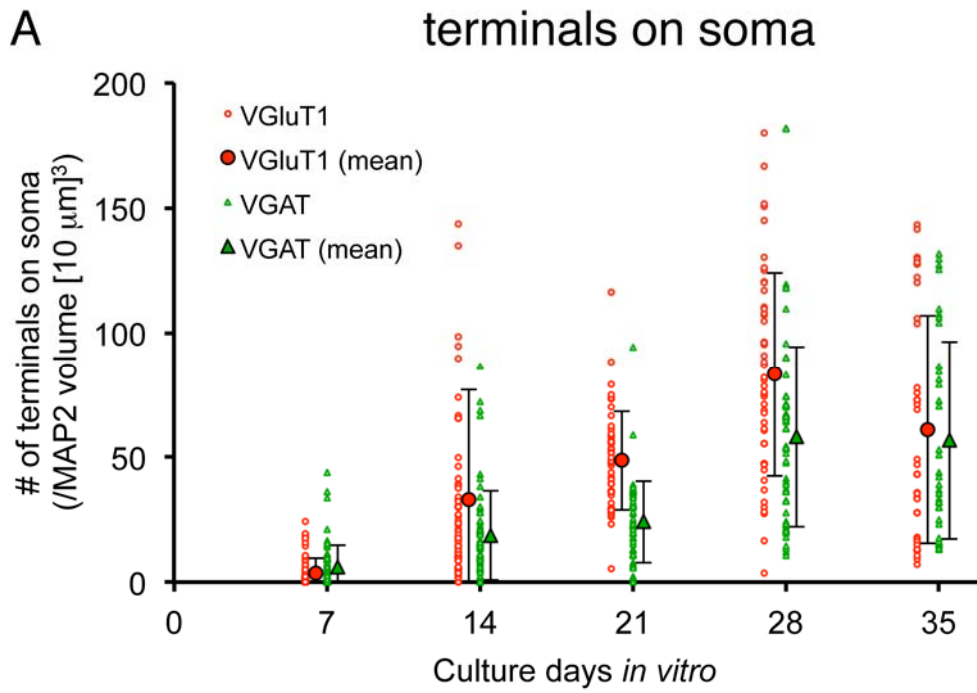


Fig. 3

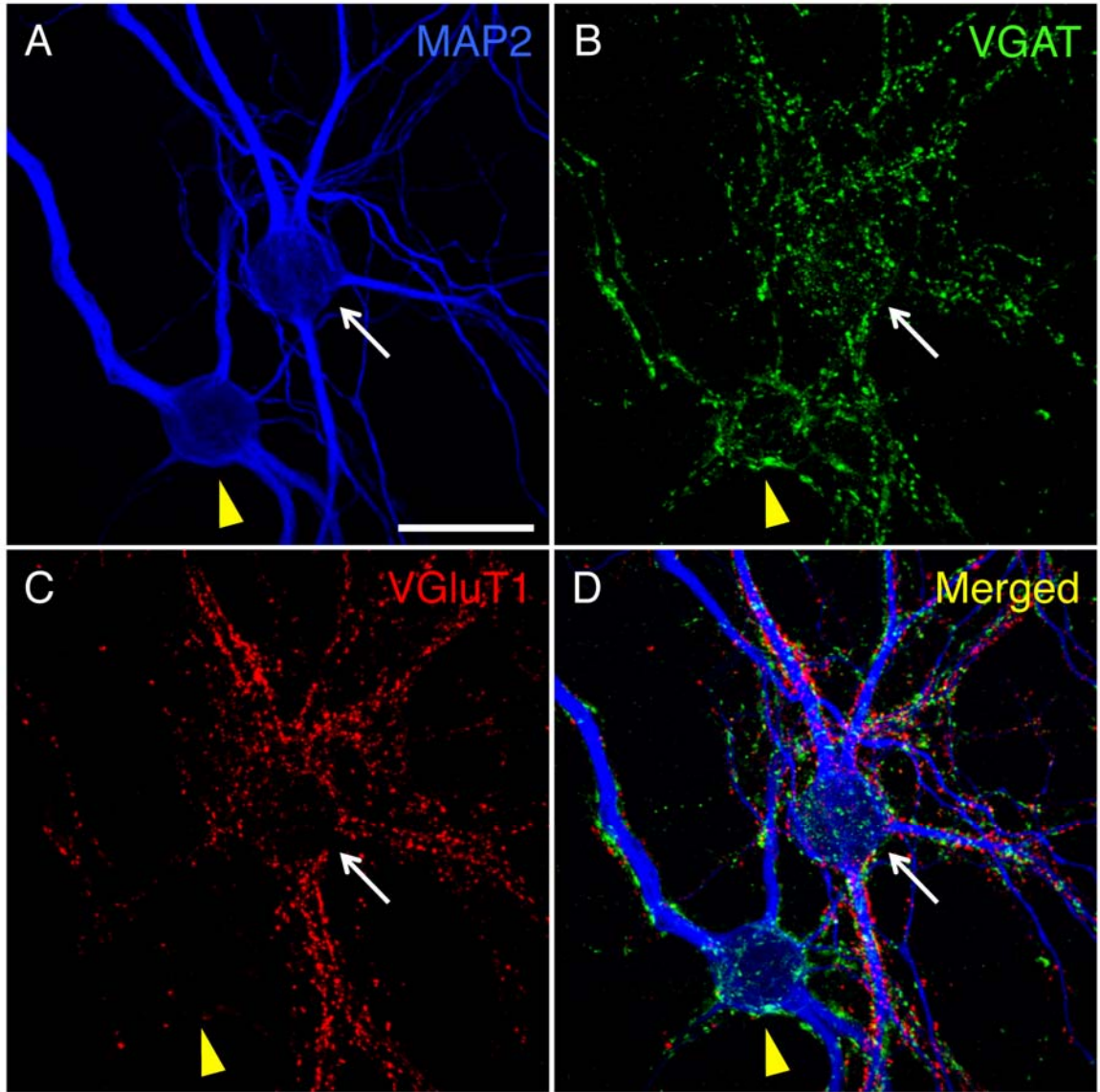


Fig. 4

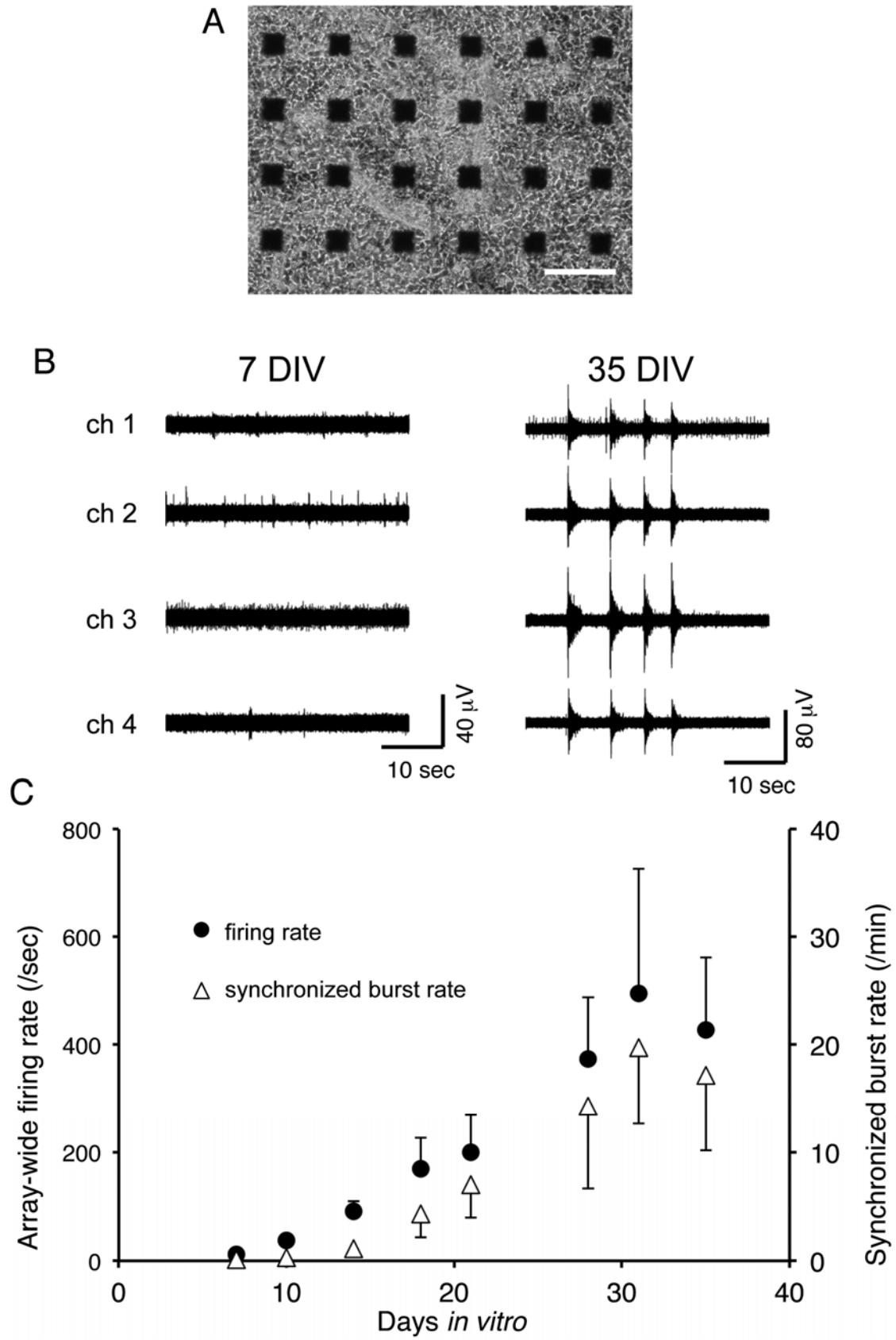


Fig. 5

compared groups		on soma		on dendrites	
		VGluT1	VGAT	VGluT1	VGAT
7 DIV	14 DIV	** $p < 0.005$	$p = 0.330$	** $p < 0.005$	$p = 0.973$
	21 DIV	** $p < 0.005$	$p = 0.051$	** $p < 0.005$	** $p < 0.005$
	28 DIV	** $p < 0.005$			
	35 DIV	** $p < 0.005$			
14 DIV	21 DIV	$p = 0.169$	$p = 0.995$	** $p < 0.005$	* $p = 0.070$
	28 DIV	** $p < 0.005$			
	35 DIV	** $p < 0.005$			
21 DIV	28 DIV	** $p < 0.005$	** $p < 0.005$	$p = 1$	** $p < 0.005$
	35 DIV	$p = 0.674$	** $p < 0.005$	$p = 1$	$p = 0.533$
28 DIV	35 DIV	* $p = 0.027$	$p = 1$	$p = 1$	$p = 0.485$

* $p < 0.05$; ** $p < 0.005$.

Table 1

compared groups	<i>p</i> value	
	on soma	on dendrites
7 DIV	$p = 1$	$p = 0.997$
14 DIV	$p = 0.204$	$*p = 0.032$
21 DIV	$**p < 0.005$	$**p < 0.005$
28 DIV	$**p < 0.005$	$**p < 0.005$
35 DIV	$p = 1$	$*p = 0.025$

$*p < 0.05$; $**p < 0.005$.

Table 2

compared groups		<i>p</i> value	
		firing rate	burst rate
7 DIV	10 DIV	$p = 1$	$p = 1$
	14 DIV	$p = 0.91$	$p = 1$
	17 DIV	$p = 0.217$	$p = 0.609$
	21 DIV	$p = 0.079$	$p = 0.080$
	28 DIV	$**p < 0.005$	$**p < 0.005$
	31 DIV	$**p < 0.005$	$**p < 0.005$
	35 DIV	$**p < 0.005$	$**p < 0.005$
10 DIV	14 DIV	$p = 0.989$	$p = 1$
	17 DIV	$p = 0.423$	$p = 0.655$
	21 DIV	$p = 0.186$	$p = 0.095$
	28 DIV	$**p < 0.005$	$**p < 0.005$
	31 DIV	$**p < 0.005$	$**p < 0.005$
	35 DIV	$**p < 0.005$	$**p < 0.005$
14 DIV	17 DIV	$p = 0.906$	$p = 0.863$
	21 DIV	$p = 0.656$	$p = 0.206$
	28 DIV	$**p < 0.005$	$**p < 0.005$
	31 DIV	$**p < 0.005$	$**p < 0.005$
	35 DIV	$**p < 0.005$	$**p < 0.005$
17 DIV	21 DIV	$p = 1$	$p = 0.935$
	28 DIV	$*p = 0.043$	$**p < 0.005$
	31 DIV	$**p < 0.005$	$**p < 0.005$
	35 DIV	$**p < 0.005$	$**p < 0.005$
21 DIV	28 DIV	$p = 0.130$	$p = 0.057$
	31 DIV	$**p < 0.005$	$**p < 0.005$
	35 DIV	$*p = 0.014$	$**p < 0.005$
28 DIV	31 DIV	$p = 0.539$	$p = 0.282$
	35 DIV	$p = 0.984$	$p = 0.986$
31 DIV	35 DIV	$p = 0.967$	$p = 0.952$

* $p < 0.05$; ** $p < 0.005$.

Table 3